Oscillating Injection Painting and Related Technical Issues

J. Beebe-Wang

June 2000

Collider Accelerator Department

Brookhaven National Laboratory

U.S. Department of Energy

DISCLAIMER

**Oscillating Injection Painting
And Related Technical Issues**

BNL/SNS TECHNICAL NOTE

NO. 081

J. Beebe-Wang

June 1, 2000

COLLIDER-ACCELERATOR DEPARTMENT
BROOKHAVEN NATIONAL LABORATORY
UPTON, NEW YORK 11973

Oscillating Injection Painting
And Related Technical Issues

Joanne Beebe-Wang

1. Introduction

Injection painting is a multi-turn injection process with a controlled phase space offset (6-D) between the centroid of injected beam and the closed orbit in the ring to achieve a different particle distribution from the injected beam. For SNS accumulator ring [1], transverse phase space painting (4-D) is decoupled from longitudinal beam manipulation (2-D). In this work, we concentrate on transverse painting only. The studies on longitudinal painting and related issues to SNS are reported separately [2].

Transverse phase space painting (4-D) will be implemented for the SNS accumulator ring injection in order to:
   A) Satisfy target requirements;
   B) Reduce beam losses due to space charge;
   C) Reduce foil hits, therefore reduce beam losses at foil and prolong foil lifetime.

For SNS injection painting, where the injection stripping foil is employed, the phase space offset is achieved by moving the closed orbit with injection bumps (x_o, x'_o) and (y_o, y'_o) as functions of time while keeping the centroid of injected beam and the injection foil stationary. There are only two basic painting methods – correlated painting and anti-correlated painting [3], as shown in Fig. 1. These are the two baseline painting schemes incorporated in the SNS accumulator ring design. Any other painting schemes are merely variation or combination of the two.

For correlated painting, illustrated by Fig. 1(a), injection begins with both (x_o, x'_o) and (y_o, y'_o) bump close to the centroid of injected beam, and gradually move away from it. So, both the emittance ε_x and ε_y of circulating beam are painted from small to large during the injection. The computer simulation shows that, with this painting scheme, the beam distribution at the extraction may satisfy the target requirements. However, such a beam profile is susceptible to transverse coupling due to magnet error/misalignment and space charge forces, which in turn makes it difficult to preserve the beam shape. Fig. 2 shows the particle distribution at the end of injection with a typical correlated painting.

For anti-correlated painting, illustrated by Fig. 1(b), bump (x_o, x'_o) moves gradually away from the centroid of injected beam, while (y_o, y'_o), moves gradually towards it. The total transverse emittance is approximately constant during the injection. The resulting oval beam

profile is immune to the transverse coupling. However, unlike correlated painting, it does not have the capability of painting over the halo/tail generated in the circulating beam with the freshly injected particles. Computer simulations show that there are always excessive halo/tails in the final distribution, which is associated with the nature of this painting scheme and cannot be corrected by bump optimization. Fig. 3 shows the particle distribution at the end of injection with a typical anti-correlated painting.

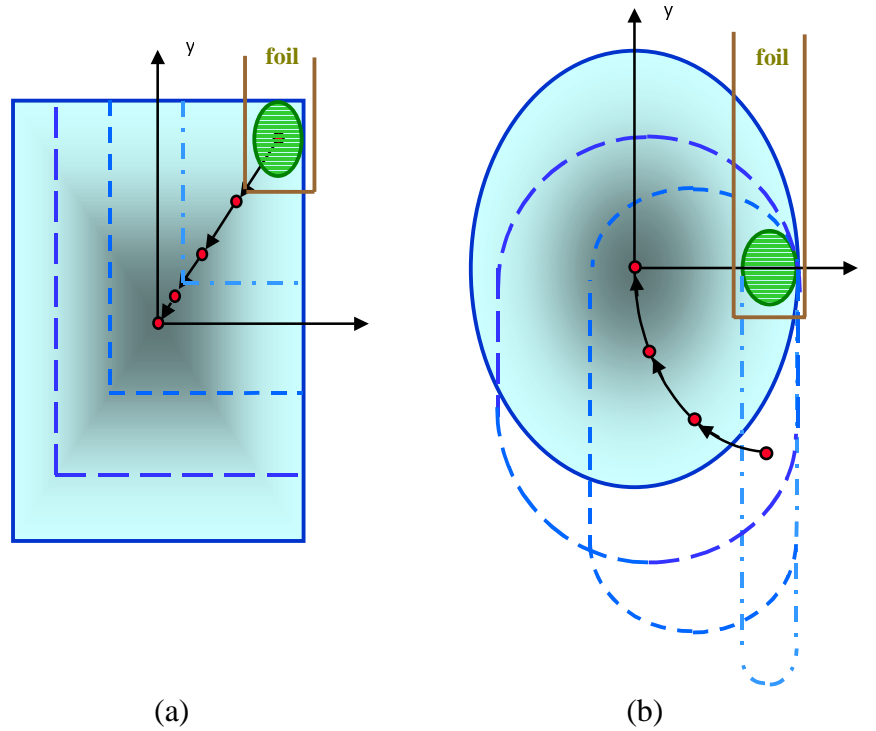(a)   (b)

Fig. 1 Illustration of basic painting methods in (x-y) space. (a) correlated painting; (b) anti-correlated painting. In both graphs, the small green ellipse represents the injected beam on the foil. The closed orbit (red dots) moves in the direction indicated by the black arrows during the injection. The beam shape and size from beginning to the end of injection are characterized by the dot-dashed, short-dashed, long-dashed and solid blue lines. The large blue-shaded rectangular and oval shapes represent the circulating beam resulting from correlated and anti-correlated painting respectively.

In order to take the advantages of both correlated and anti-correlated painting and over come with their disadvantages, a new painting scheme was proposed at BNL [4]. It is a combination of anti-correlated and reverse anti-correlated painting with slowly increasing amplitude. With this painting scheme, closed orbit moves as an anti-correlated painting, with smaller amplitude, in a time period $(0, t_{inj})$. Here $t_{inj} = \tau_{inj}/n$ which is a fraction $1/n$ of injection time τ_{inj}. So, the beam reaches KV-like distribution with a smaller emittance at time t_{inj}. In the next time period $(t_{inj}, 2t_{inj})$, the closed orbit oscillates back as a reversed anti-correlated painting with slightly increased amplitude. So, the beam reaches a KV-like distribution again at time $2t_{inj}$

with a slightly larger emittance. Repeating the anti-correlated painting in the 3rd, 5th, 7th ... time period, and reverse anti-correlated painting in the 4th, 6th, 8th ... time period, we obtain a KV-like distribution at the end of each time period with a slightly larger emittance than the one before. If the amplitude increases with the same rate as the emittance growth due to space charge, at the end of injection time τ_{inj} , we obtain a beam distribution with less tail/halo than the ones from anti-correlated or reverse anti-correlated painting alone. This new painting technique will be called the "oscillating painting scheme".

Fig. 2 The particle distribution at the end of injection with a typical correlated painting. The result from computer simulation including space charge is represented by red dots/lines, which should be compared to the one without space charge represented by blue dots/lines. The top left and right figures show the particle distributions in (x, x') and (y, y') phase space respectively. The bottom left and right figures show the distribution in (x, y) space and the distribution of 4-D phase space areas occupied by single particles in the circulating beam.
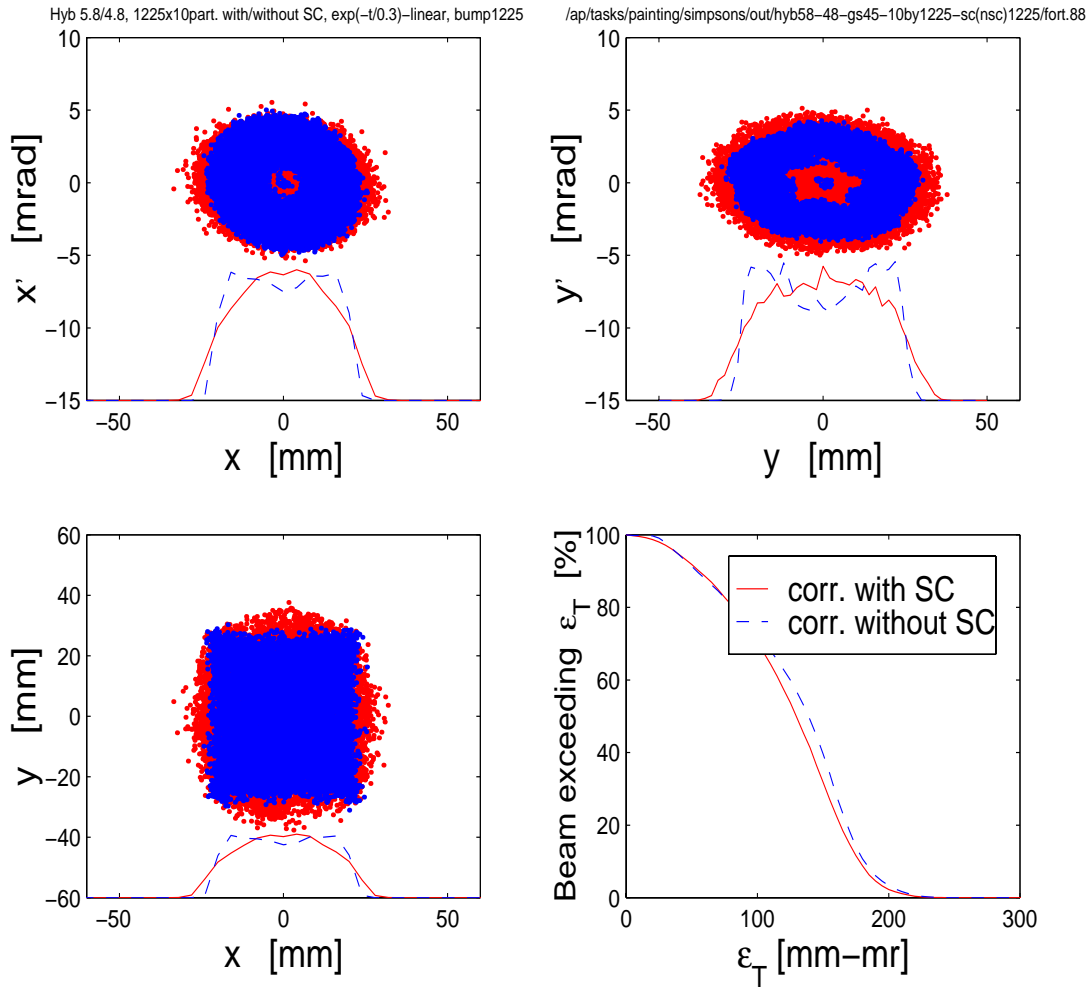
Fig.3   The particle distribution at the end of injection with a typical anti-correlated painting. The result from computer simulation including space charge is represented by red dots/lines, which should be compared to the one without space charge represented by blue dots/lines. The top left and right figures show the particle distributions in (*x, x'*) and (*y, y'*) phase space respectively.   The bottom left and right figures show the distribution in (*x, y*) space and the distribution of 4-D phase space areas occupied by single particles in the circulating beam.
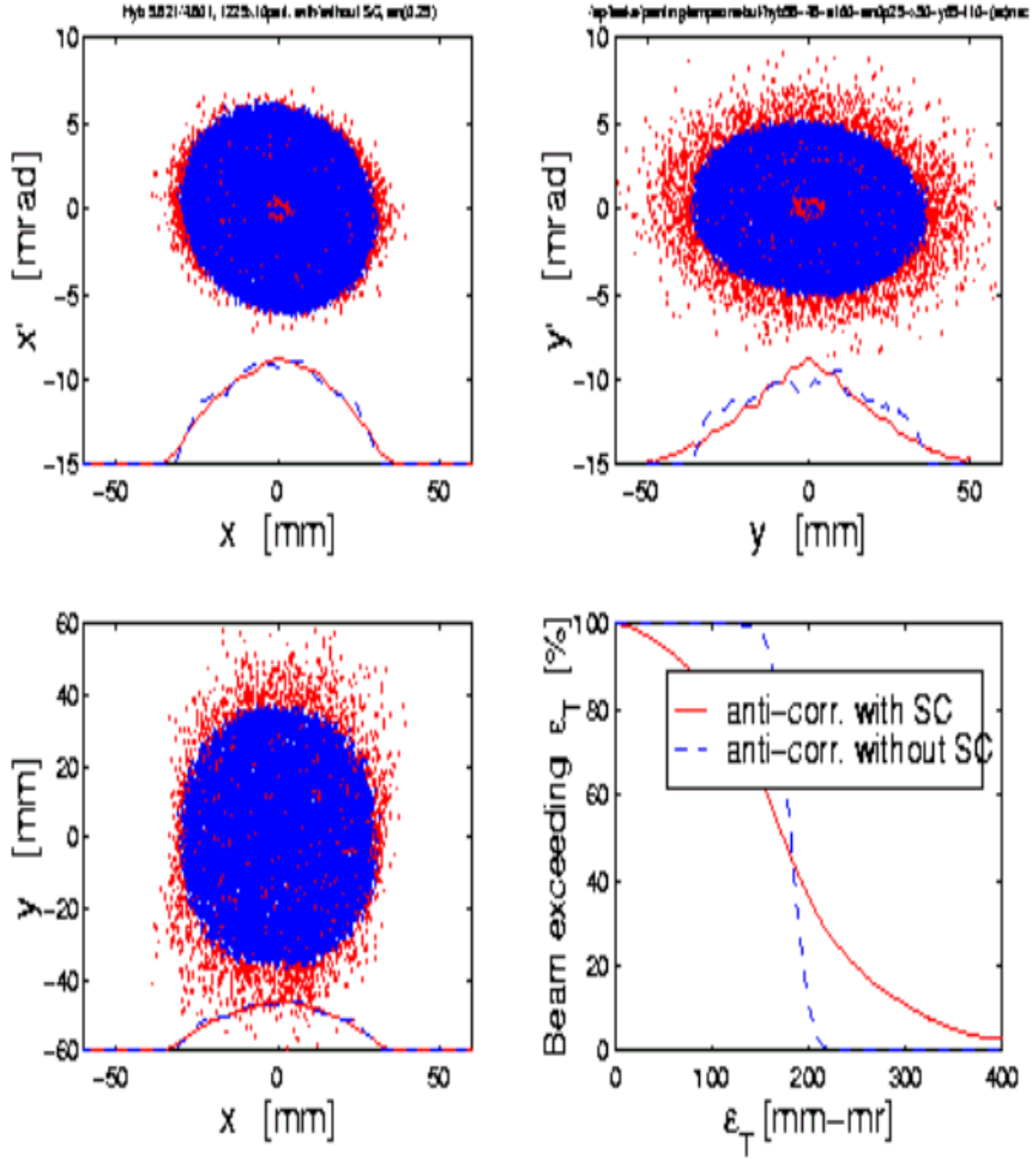
2. Analytical Expression

Here we derive an analytical expression of (x, y) space distribution resulting from oscillating painting neglecting space charge effects. We will present simulation studies including space charge in the next section. Transverse phase space painting is a 4-D problem (x, x', y, y'). But, if the distribution of injected beam can be expressed as

$$n_0(x, x', y, y') = n_{0x}(x, x') \, n_{0y}(y, y') \tag{1}$$

and the bump in (x, x') phase space moves independently from phase space (y, y'), the 4-D problem could reduce to a 2-D by 2-D problem. Therefore, we can solve a 2-D phase space problem first, then superimpose the solution in (x, x') onto the one in (y, y') to get the 4-D phase space expression. The justification of this assumption and other assumptions used in the following will be given at the end of this section.

We first consider a single particle injected into the ring at the location of foil with initial phase space coordinates $P=(x_0, p_{x0}')$, where $p_x = \alpha_x x + \beta_x x'$. Upon subsequent revolutions around the ring, this particle reappears at the location of the foil with phase space coordinates $=(x, p_x')$. The particle motion in parameterized 2-D phase space is

$$x - X_o(t) = a_x(t)\cos(\omega_x t + \varphi_x) \tag{2}$$

$$p_x - P_{xo}(t) = a_x(t)\sin(\omega_x t + \varphi_x) \tag{3}$$

where $(X_o(t), P_{xo}(t))$ is the location of closed orbit at time t, and

$$a_x(t) = \left\{ [x_o - X_o(t)]^2 + [p_{xo} - P_{xo}(t)]^2 \right\}^{1/2} \tag{4}$$

$$\varphi_x = \tan^{-1} \frac{P_{xo} - P_{xo}(t)}{x_o - X_o(t)} . \tag{5}$$

At any given time t, the probability of finding this particle at location (x, p_x) is:

$$f_{one,x}(x, p_x) = \delta_x \left\{ [x - X_o(t)] - a_x(t)\cos(\omega_x t + \varphi_x) \right\} \delta_y \left\{ [p_x - P_{xo}(t)] - a_x(t)\sin(\omega_x t + \varphi_x) \right\}. \tag{6}$$

If $a_x(t)$ changes slowly compared to betatron oscillation, the particle distribution in (x, p_x) phase space can be obtained by integration over one circulation period:

$$f_{one,x}(x, p_x) = \frac{1}{\pi \left\{ a_x^2(t) + [x - X_o(t)]^2 \right\}^{1/2}} \delta_y \left\{ [p_x - P_{xo}(t)] - \left\{ a_x^2(t) + [x - X_o(t)]^2 \right\}^{1/2} \right\} . \tag{7}$$

Clearly, particles injected at P paint the same phase space as particles injected at P_1 regardless of phase φ_x. Maximum ε_x is determined by the particles injected at Q (see Fig.4).

Substituting (x, p_x) by (y, p_y), (X_0, P_{X0}) by (Y_0, P_{Y0}), and $a_x(t)$ by $a_y(t)$, we also obtain a similar expression in (y, p_y) phase space. Integrating over p_x and p_y, the one particle distribution in (x, y) real space at time t is given by:

$$n(x, y, t) = \frac{1}{\pi^2 \left[a_x^2(t) - (x - X_o(t))^2 \right]^{1/2} \left[a_y^2(t) - (y - Y_o(t))^2 \right]^{1/2}} \tag{8}$$
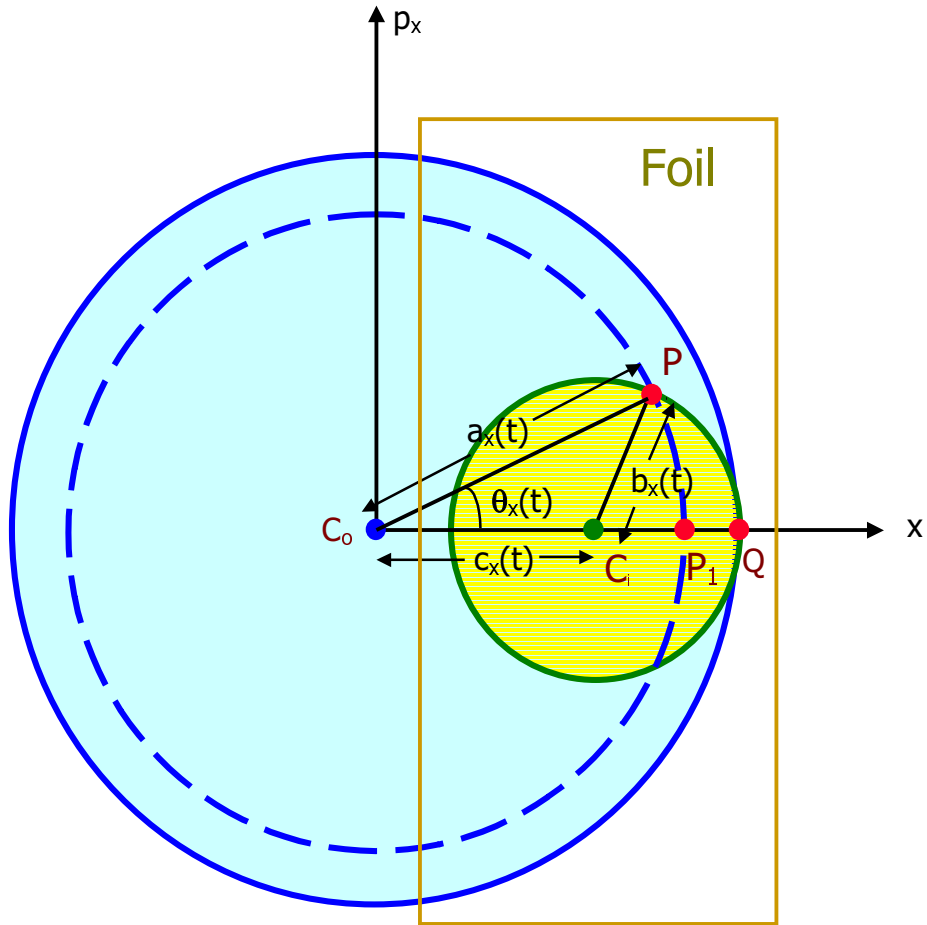

Fig.4 Illustration of injection painting in (x, p_x) phase space.

Now consider that the injected beam distribution is Gaussian with σ_x and σ_y. In order to simplify the problem, we transfer the 2-D phase space coordinates into the one shown in Fig. 4. In these coordinates, the closed orbit of the circulating beam $C_o(t)=(X_o(t),P_{Xo}(t))$ is at the reference point, and the centroid of injected beam $C_i=(X_i , P_{xi})$ is on the x-axis. The effective 2-D phase space offset between the two centers is:

$$c_x(t) = \{\Delta X^2(t) + [\beta_x \Delta X'(t) + \alpha_x \Delta X(t)]^2\}^{1/2} \quad , \qquad (9)$$

where $\Delta X = X_i - X_o(t)$ and $\Delta X' = X'_i - X'_o(t)$.

Integrating entire particle distribution of injected beam, the circulating beam distribution in (x, y) space at time t is given by [5]:

$$n(x, y, t) = \int_0^t n_x(x,t_1)n_y(y,t_1)dt_1 \qquad (10)$$

$$n_x(x,t_1) = \frac{1}{\pi\sigma_x^2} \int_{|x|}^{+\infty} e^{-\{[a_x - c_x(t_1)]^2/2 + |a_x c_x(t_1)|\}/\sigma_x^2} \frac{a_x I_0\left(\dfrac{a_x c_x(t_1)}{\sigma_x^2}\right)}{(a_x^2 - x^2)^{1/2}} da_x \quad , \qquad (11)$$

where $I_0(z)$ is the modified Bessel function of order zero. In the above expression $n_y(y, t_1)$ can be obtained from $n_x(x, t_1)$ by replacing x by y.

A KV-like distribution at time t_{inj} may be obtained by carefully design injection bump motion in 4-D phase space:

$$\Delta X(t) = A\left(\frac{t}{t_{inj}}\right)^{1/2} \qquad (12)$$

$$\Delta X'(t) = -A\left(\frac{t}{t_{inj}}\right)^{1/2}\frac{\alpha_x}{\beta_x} \qquad (13)$$

$$\Delta Y(t) = B\left(1 - \frac{t}{t_{inj}}\right)^{1/2} \qquad (14)$$

$$\Delta Y'(t) = -B\left(1 - \frac{t}{t_{inj}}\right)^{1/2}\frac{\alpha_y}{\beta_y} \qquad (15)$$

If $\sigma_x << \Delta X(t)$, $a_x(t)$ and $\sigma_y << \Delta Y(t)$, $a_y(t)$, we can keep only the zero and first order of σ_x and σ_y in Equ. (11). The real space distribution (Equ.(10)) at time $t=t_{inj}$ becomes:

$$n(x, y, t_{inj}) = f_0(x, y) + f_1(x, y) \tag{16}$$

with the zeroth order:

$$f_0(x, y) = \begin{cases} \dfrac{t_{inj}}{\pi AB} & for \dfrac{x^2}{A^2} + \dfrac{y^2}{B^2} \leq 1 \\ 0 & for \dfrac{x^2}{A^2} + \dfrac{y^2}{B^2} > 1 \end{cases} \tag{17}$$

and first order:

$$f_1(x, y) = -\frac{\sqrt{2}\,t_{inj}}{\pi^{5/2} AB} \left\{ \frac{\sigma_x}{A\zeta} \left[F(\frac{\pi}{2}, \psi) - F(0, \psi) + \frac{x^2}{A^2\zeta^2\psi} \left(\Pi(\frac{\pi}{2}, \psi^2, 1) - \Pi(0, \psi^2, 1) \right) \right] \right.$$
$$\left. \frac{\sigma_y}{B\eta} \left[F(\frac{\pi}{2}, \xi) - F(0, \xi) + \frac{x^2}{B^2\eta^2\xi} \left(\Pi(\frac{\pi}{2}, \xi^2, 1) - \Pi(0, \xi^2, 1) \right) \right] \right\} \tag{18}$$

where $\eta = \sqrt{1 - \dfrac{x^2}{A^2}}$, $\zeta = \sqrt{1 - \dfrac{y^2}{B^2}}$, $\xi = \dfrac{1}{\eta}\sqrt{1 - \dfrac{x^2}{A^2} - \dfrac{y^2}{B^2}}$, $\psi = \dfrac{1}{\zeta}\sqrt{1 - \dfrac{x^2}{A^2} - \dfrac{y^2}{B^2}}$

and F is the elliptic integral of the first kind and Π is the elliptic integral of the third kind.

We obtain a true KV distribution $f_0(x,y)$ at time $t=t_{inj}$ with zeroth order approximation ($\sigma_x=\sigma_y=0$),. When the first and higher orders of σ_x and σ_y are included we obtain a KV-like distribution, as long as $\sigma_x << c_x(t)$ and $\sigma_y << c_y(t)$. If we reverse the bump motion during the next time period (t_{inj}, $2t_{inj}$) we will again obtain a KV-like distribution at time $t=2t_{inj}$. So, as described in Section 1, by oscillating the bump we obtain a KV-like distribution at the end of injection ($t=\tau_{inj}=nt_{inj}$).

In the derivation of the analytical expression above four assumptions have been made. In the following these assumptions are stated and are justified for the SNS injection criteria:
   (1) The complete painting is a 6-D problem. We study transverse (4-D) painting and assume that longitudinal painting (2-D) can be investigated separately. Since the beam is injected into the SNS ring at a dispersion-free region [1], the transverse phase-space painting is conveniently de-coupled from the longitudinal beam manipulation [2]. In addition, the coupling between particle longitudinal and transverse motion is small due to the large difference between the synchrotron frequency and betatron frequency.
   (2) The transverse painting is a (4-D) problem. We assume this 4-D problem can be reduced to a 2-D by 2-D problem. In the present injection design [1], the horizontal and vertical bumps are formed by two sets of four pulsed dipoles. Programmable power supplies control the strengths of the dipoles in each direction, independently. Furthermore, the injected beam has 4-D Gaussian distribution, which satisfies Equ. (1).

(3) We have assumed that the bumps move slow compared to betatron oscillation. It is true for SNS injection since $<|dx/dt|>|_{bump} = 40$m/sec and $<|dx/dt|>|_{beta} = 1 \times 10^6$m/sec.

(4) We have also assumed σ_x and σ_y are small compared to the offset between the centroid of injected beam and the closed orbit in 2-D phase space: $\sigma_x \ll c_x(t)$ and $\sigma_y \ll c_y(t)$. These are true most of the time for the SNS injection, except at very beginning and very end of each time period $[(k-1)t_{inj}, kt_{inj}]$, $k=0, 1, 2...n$.

3. Simulation Results

It was shown in the last section that a KV-like distribution is obtained by moving the bumps as functions of time given by Equs. (12)-(15), which is technically difficult to produce. However, it can be proven mathematically that KV-like distribution will be maintained if the bump motion does not differ from Equs. (12)-(15) much. Fig. 5 compares square root bumps, Equs. (12)-(15), with exponential bumps (τ=0.5 and 0.6msec) and sinusoidal bumps.
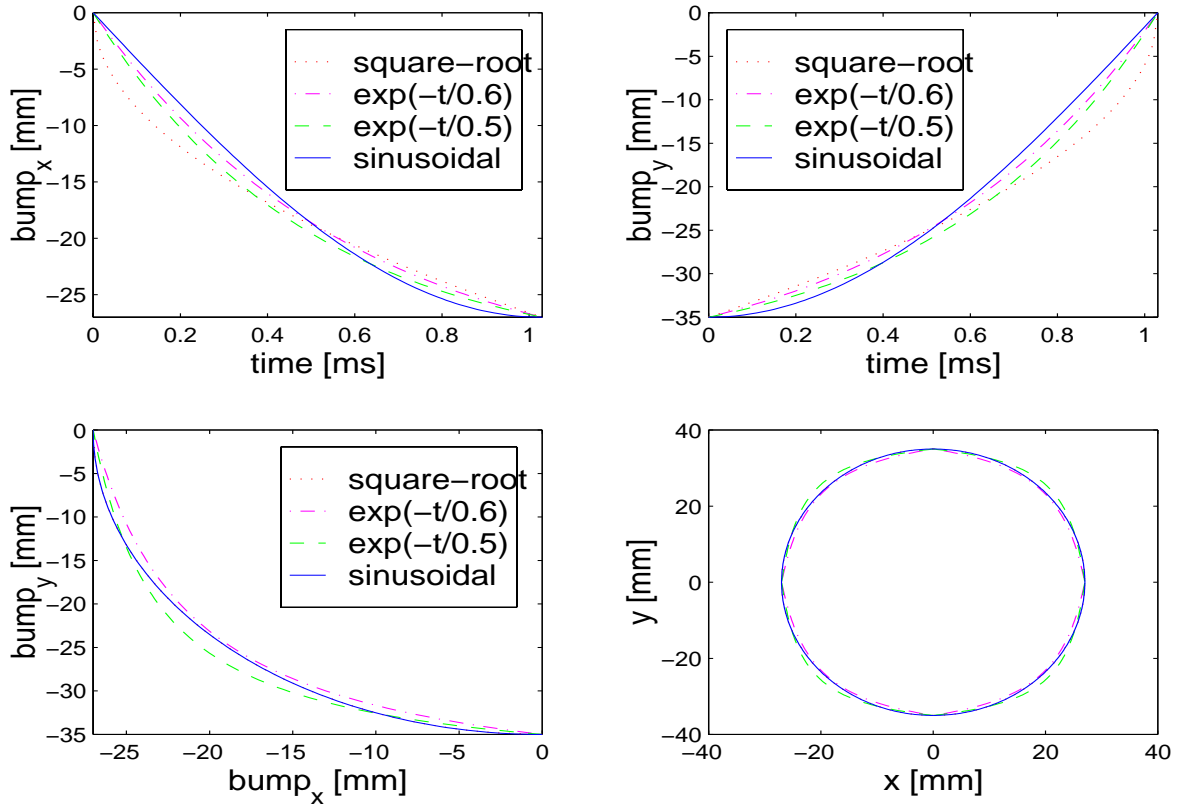

Fig. 5 Comparison of injection bumps and resulting beam shapes. The bumps with square root functions, Equs. (12)-(15), shown by red dotted lines are compared with other kinds of bumps: (a) exponential bump with time constant τ=0.6msec (red dot-dashed lines); (b) exponential bump with time constant τ=0.5msec (green dashed lines) and (c) sinusoidal bump (blue solid lines).

It has been demonstrated by computer simulations that Equs. (12)-(15) maybe replaced by a sinusoidal function with carefully chosen parameters, which will make it easier to control the bump technically without loss the physical characteristics. The amplitude of this sine bump should be slowly increased during the injection, which insures the freshly injected particles be able to paint over halo/tail. The simplest form is that amplitude increases linearly as function of time:

$$\Delta X_b(t) = \left[(1 - f_x)\frac{t}{\tau} + f_x\right]\left[\Delta X_{min} + (\Delta X_{max} - \Delta X_{min})\left|\sin(\omega_{bx}t)\right|\right] \tag{19}$$

$$\Delta X'_b(t) = -\Delta X_b(t)\frac{\alpha_x}{\beta_x} \tag{20}$$

$$\Delta Y_b(t) = \left[(1 - f_y)\frac{t}{\tau} + f_y\right]\left[\Delta Y_{min} + (\Delta Y_{max} - \Delta Y_{min})\left|\cos(\omega_{by}t)\right|\right] \tag{21}$$

$$\Delta Y'_b(t) = -\Delta Y_b(t)\frac{\alpha_y}{\beta_y}\quad. \tag{22}$$

The *x*-bump (Equ. (19)) and *y*-bump (Equ.(21)) for 3 different oscillating paintings with $f=f_x=f_y$=0.5, 0.8 and 1.0 are shown in Fig. 6. Note f=1.0 is a special case of oscillating painting without amplitude increase.
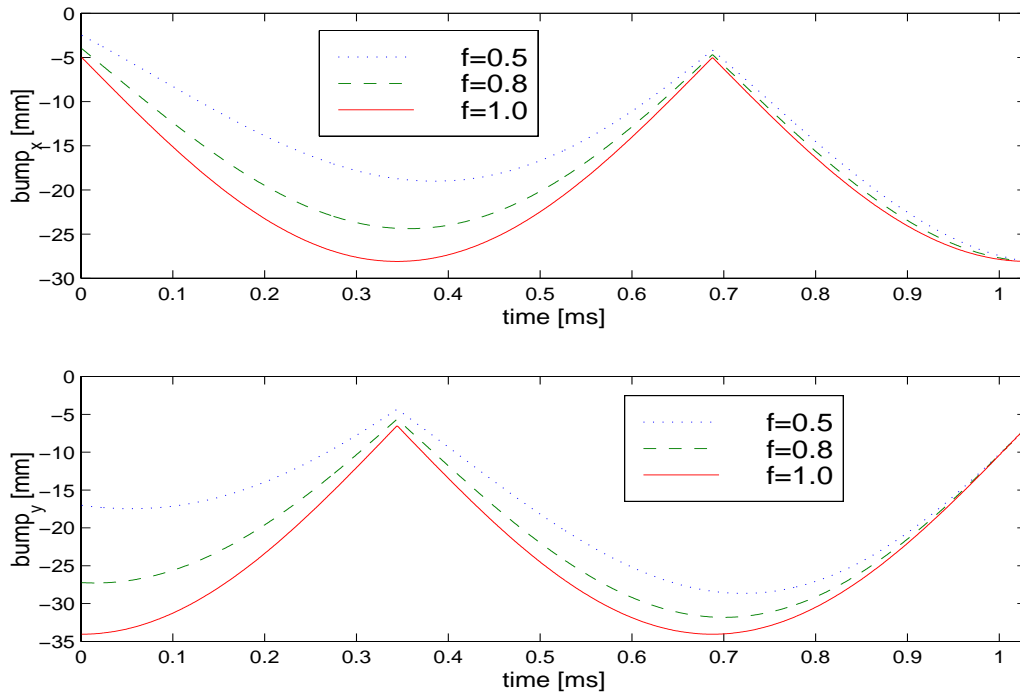

Fig. 6 The *x*-bump (Equ. (19)) and *y*-bump (Equ.(21)) for 3 different oscillating paintings with $f=f_x=f_y$=0.5, 0.8 and 1.0 respectively.

The simulations are performed with SIMPSONS [6] including space charge, magnet errors and misalignments. All the physical parameters are chosen as close as possible to the design specification [7]. Considering the degree of technical difficulty imposed on power supplies, the bump oscillation frequency is chosen so that, during entire injection time, we choose $t_{inj} = \tau_{inj}/n$, $n=3$ which is the minimum to see the oscillation effect. Figs. 7 and 8 show particle distributions at the end of injection with oscillating painting governed by Equs. (19)-(22) With $f=f_x=f_y=0.5$ and 0.8 respectively.
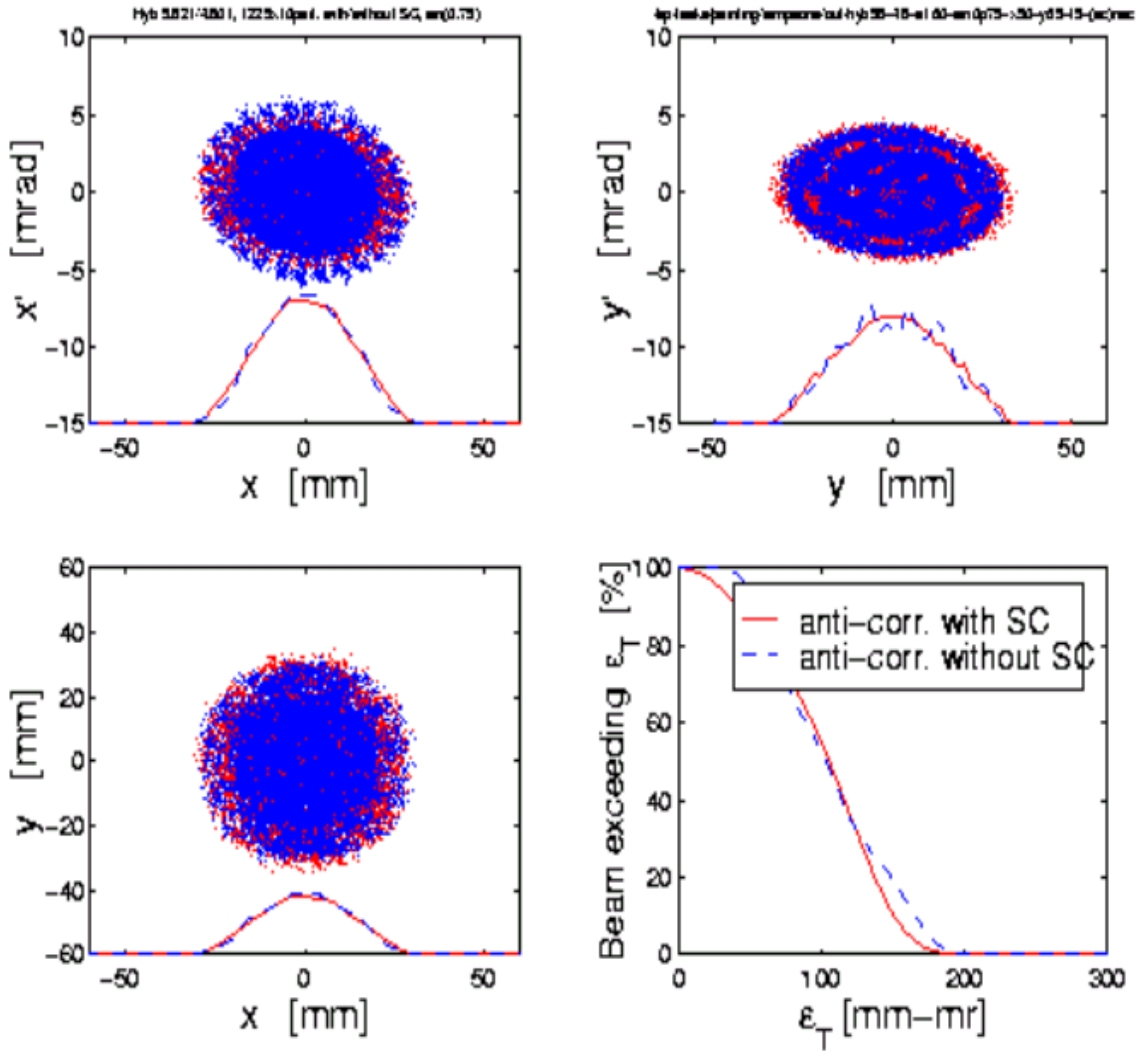
Fig.7 Oscillating painting with $f=f_x=f_y=0.5$ resulting a distribution with no halo/tail but less uniform. The result from computer simulation including space charge is represented by red dots/lines, which should be compared to the one without space charge represented by blue dots/lines. The top left and right figures show the particle distributions in (x, x') and (y, y') phase space respectively. The bottom left and right figures show the distribution in (x, y) space and the distribution of 4-D phase space areas occupied by single particles in the circulating beam.

All the physical and numerical parameters in the simulations with oscillated painting are kept same as the anti-correlated painting presented in Fig. 3, except $n=3$ instead $n=1$. Comparing oscillating painting (Fig. 7 and 8) with anti-correlated painting (Fig. 3), it can be easily observed that oscillating painting can largely reduce the undesirable halo/tail in the final distribution. The amount of the halo/tail reduction depends on the speed of amplitude increase in the sine function. The smaller the f value is, the faster bump amplitude increases, therefore, the less halo/tail in the final distribution. The trade-off is a less uniform distribution. Fig. 7 demonstrates an oscillating painting with more amplitude increase (f=0.5) resulting a distribution with no halo/tail but less uniform. While Fig. 8 gives more uniform distribution, but has some halo/tail, obtained from an oscillating painting with less amplitude increase (f=0.8).
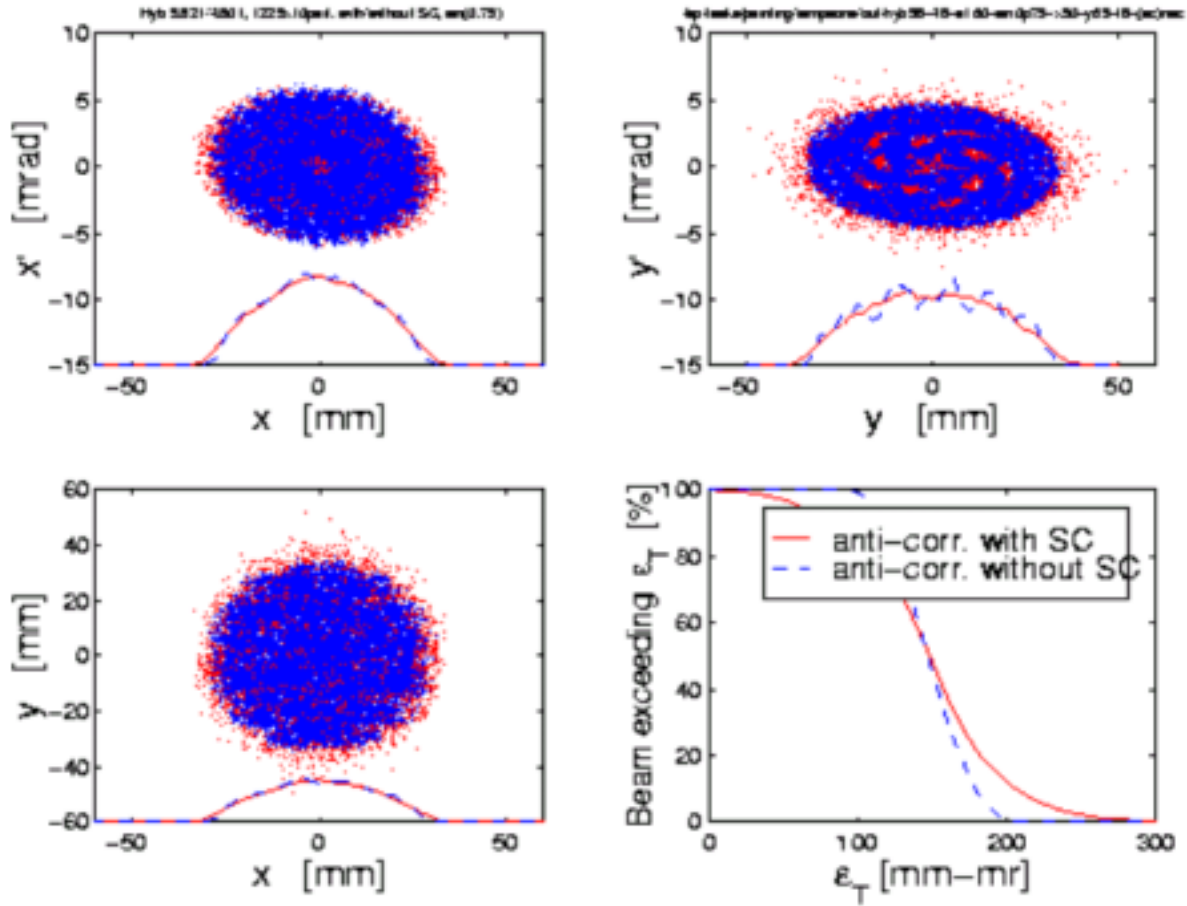
Fig.8   Simulation results of oscillating painting with $f=f_x=f_y=0.8$ resulting more uniform distribution, but has some halo/tails.   The result from computer simulation including space charge is represented by red dots/lines, which should be compared to the one without space charge represented by blue dots/lines.   The top left and right figures show the particle distributions in (x, x') and (y, y') phase space respectively.   The bottom left and right figures show the distribution in (x, y) space and the distribution of 4-D phase space areas occupied by single particles in the circulating beam.

4. Technical Issues

Aperture

An aperture larger than the final beam emittance may be needed if the painting is obtained by moving the closed orbit instead of moving the centroid of injected beam. Due to the large emittance in the (y, y') phase space at the beginning of the injection, anti-correlated painting requires an aperture of 150% of full beam emittance in the y-direction. Similarly, reverse anti-correlated painting requires an aperture of 150% of full beam emittance in the x-direction. Since an oscillating painting is a combination of anti-correlated and reverse anti-correlated painting, it requires 150% of full beam emittance in both x- and y-directions. Table 1 summarizes the aperture requirements of the painting schemes, where Δ_H and Δ_V denote horizontal and vertical full beam clearance respectively.

The apertures in SNS accumulator ring are designed to accommodate correlated and anti-correlated painting schemes. But, due to injection layout, there is not enough horizontal aperture for reverse anti-correlated painting and oscillating painting. However, since the bump amplitudes increase during the injection, full aperture is not needed until the end of injection. So, it may still be possible, with carefully chosen bump functions, to implement oscillating painting with a smaller aperture.

Table 1 Aperture requirements of the painting schemes.

Painting Schemes	Aperture Requirment	
	Horiz. Δ_H [%]	vert. Δ_V [%]
Correlated	100	100
Anti-corr.	100	150
Rev. anti-corr.	150	100
Oscillated	150	150

Power Supplies

Programmable Power Supply

The 4-D transverse injection paintings, as we described above, require dynamic bumps in both horizontal and vertical directions. Each dynamic bump consists of 4 kickers. For SNS accumulator ring theses kickers are IkickH9A, 9B, 13A 13B (horizontal), and IkickV9A, 9B, 13A 13B (vertical). Due to the sophisticated current waveforms imposed by stringent particle distribution requirement, the power supplies need to be programmable. For correlated and anti-correlated painting, the power supplies also need to have:

(a) Power rating ranges from 100V/110A to 800V/1400A;
(b) 2kHz Bandwidth;
(c) Load current tracking error <5%;
(d) Initial and final load current error <1%;
(e) Time constant for load current raise/fall <0.3msec.

In order to study the current response in the kicker magnet coil, a computer simulation was performed with designed parameters (coil resistance $=3.02\text{m}\Omega$, coil inductance$=158.2\mu\text{H}$) [8]. When the desired exponential waveform with time constant $\tau=0.3\text{ms}$ (the red dash-doted line in top graph of Fig. 9) is fed into the power supply as a reference current, it responds with the load current in coil (the green solid line in top graph of Fig. 9). This load current is obtained by setting the programmable voltage to be $V_{max}=440\text{V}$ (green solid line in bottom graph of Fig. 9). Obviously, there is a significant delay in the coil current response, which does not meet the above requirement. However, we can produce output load currents close to desired waveforms by empirically adjusting the input reference functions. The blue dashed lines in Fig. 9 show an example of load current (top graph) and corresponding voltage $V_{max}=600\text{V}$ (bottom graph) obtained by an input reference exponential waveform with $\tau=0.2\text{ms}$. It seems reasonable to expect a load current be within 5% error to desired current, as long as it falls between the blue and green lines. Based on simulation results, a programmable power supply can basically produce the waveforms required by correlated and anti-correlated painting.

However, it was found by computer simulations [9] that, in order to obtain 1.5 oscillations, the requirement on a programmable power supply is 2000V and 1300A with bandwidth 2kHz. Programmable power supplies, typically use two types of current regulation. The first kind is linear power supply that uses a linear (transistor or IGBT bank) regulator. The most up-to-date linear power supply that industry currently produces has bandwidth of 2kHz, but the maximum voltage is about 1000V. The second kind is switching power supply that uses IGBT switching modules. This kind of power supply may be capable of providing the voltage and current needed, but it is challenging to meet the bandwidth requirement. It seems that, with the current technology, a programmable power supply could not support oscillating painting [9, 10]. See Appendix for detailed waveform analysis.
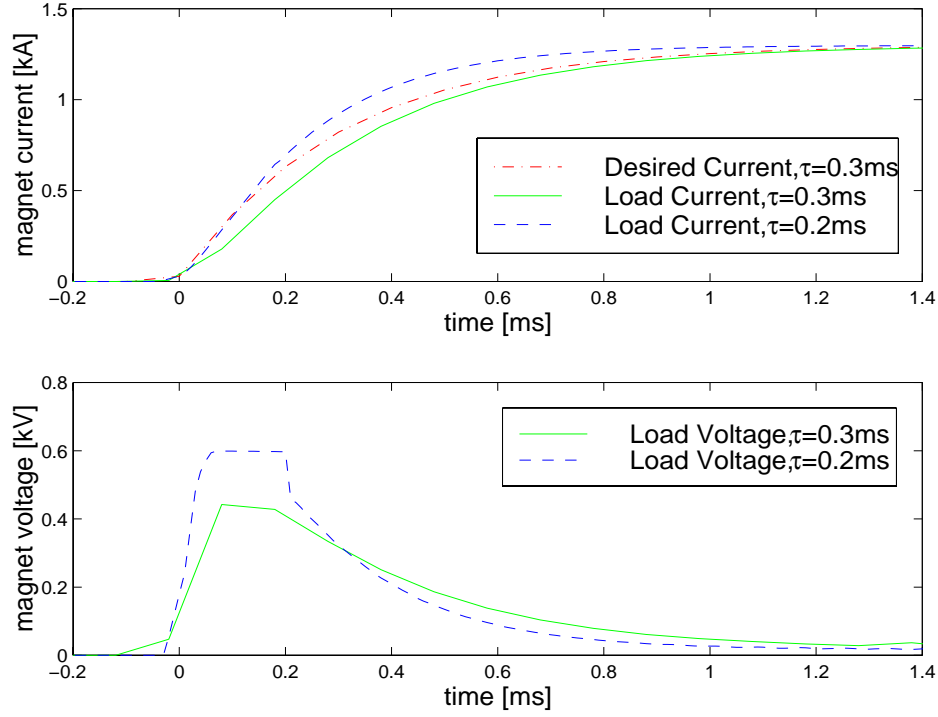
Fig. 9 Computer simulation of current response (top graph) in the kicker magnet coil and the corresponding voltage (bottom graph). The red dash-doted line is one of desired exponential waveforms with time constant τ=0.3ms. The green solid lines are coil current (top) and the corresponding voltage (bottom) responding to reference current τ=0.3ms. The blue dashed lines are coil current (top) and the corresponding voltage (bottom) responding to reference current τ=0.2ms.

High-Q resonant power supply

A high–Q resonant power supply for oscillated painting is under development in BNL. Such power supply needs to meet the following requirements:

    (a) Produce waveforms of rectified sine-functions with minimum frequency of 750Hz;
    (b) Q>20;
    (c)   2kHz Bandwidth;
    (d) Load-current tracking error <5%.

It is technically challenging to build such power supply, and it requires better electrical insulation for injection kicker magnets. Presently, the capability of accommodating oscillating painting for SNS injection is unknown.

5. Discussion and Conclusions

Oscillating painting scheme combines the advantages of both correlated and anti-correlated painting. It has the capability of painting over the halo/tails generated in the circulating beam with the newly injected particles; meanwhile, the resulting KV-like distribution is immune to the transverse coupling. However, it requires larger aperture and higher output rating power supply.

At present, the most advanced programmable power supply cannot accommodate oscillating painting for SNS injection. A High–Q resonant power supply is currently under development. Due to the technical challenges, its capability to accommodate oscillating painting for SNS injection remains unknown.

However, Oscillating painting could be a good painting scheme for the other facilities where injection time is longer (for example, 5msec) and/or magnet inductance is lower (for example 30μH). Also, output rating of power supplies has been improved every year along with the increased demand and development of modern technology. In the future, it is conceivable to have oscillating painting for SNS injection if considerable resources are expended for power supply development.

6. Reference

[1] SNS Project Office, "Spallation Neutron Source Design Manual" (1998).
[2] Joanne Beebe-Wang, "Study of Longitudinal Injection/stacking in the SNS Accumulator Ring", p. 2843, Proc. of PAC99 (1999).
[3] Joanne Beebe-Wang *et al*, "Transverse Phase Space Painting For SNS Accumulator Ring Injection", p. 1743. Proc. of PAC99 (1999).
[4] Joanne Beebe-Wang, research notes, BNL, Oct. 1999.
[5] D. A. Edwards and M. J. Syphers, "An introduction to the Physics of High Energy Accelerators", John Wiley & Sons, Inc., (1993).
[6] S. Machida, "The Simpsons User's Manual", Dallas, 1992.
[7] SNS Project Office, "SNS Parameter List", SNS-100000000-PL0001-R02 (2000).
[8] Wahfun Eng, Private communications, BNL, April 2000.
[9] Wahfun Eng, Private communications, BNL, March 30, 2000.
[10] Andy Soukas, Private communications, BNL, Oct. 15, 1999;
   Jon Sandberg, Private communications, BNL, March 28, 2000.

7. Appendix

INJECTION KICKER P. S. WAVEFORM ANALYSIS   Wahfun Eng   March 30, 2000

The Injection Kicker power supply is rated at 1300A with a voltage bipolar output of +150V, -800V. When a rectified 500 Hz sinewave (see diagram below) is fed into the power supply, the load current follows the input closely. The load voltage is found to be about 640 volts peak to peak (Load = 3 mΩ + 158 μH). Unfortunately, the proposed reference has a frequency about 1.33 KHz, which is about 2.7 times higher. With this reference, the voltage across the load will be 1728 volts peak to peak. To handle this, the power supply must now have a bipolar output of +/- 875V. Power supplies with this kind of output ratings are fairly limited. For one thing, no linear (transistor bank) power can handle this, which means that switching power supply is the only remaining candidate. The required 2k Hz or more bandwidth, however, is hard to do with a switching power supply.

VLoad, ILoad & Ref. vs TIME in sec.